**JURNAL SAINS MATERI INDONESIA (JUSAMI)**
ISSN: 1411-1098 (print), 2614-087X (online)
VOL. 25, ISSUE 2, 2024
DOI:10.55981/jsmi.2024.924

**ORIGINAL ARTICLE**

# Adsorption Study of Methylene Blue and Methyl Red on Activated Carbon from Silver Composite Using the Extract of Spent Coffee Grounds

H. S. Rafidah[1], H. Prasetia[2,*] and A. Saefumillah[1]

[1]Department of Faculty of Mathematics and Natural Sciences, Universitas Indonesia, Depok 16424, Indonesia
[2]Research Center for Chemistry, National Research and Innovation Agency (BRIN), South Tangerang 15314, Indonesia

**ABSTRACT** – The activated carbon was prepared from silver composite via an extract of spent coffee grounds with phosphoric acid activation. The activated carbon was used to study the removal of methylene blue and methyl red from an aqueous medium. Fourier-transform infrared spectroscopy (FTIR) spectra confirmed the functional group of O–P–O that can interact with dye molecules and the reduction process of $Ag^{+}$ to $Ag^{0}$. Field Emission Scanning Electron Microscopy (FESEM) morphology suggests a porous and irregular polygonal shape. The efficiency removal and adsorption capacity of methylene blue reached 98.73% and 9.87 mg/g at pH 9, while methyl red reached 98.55% and 9.86 mg/g at pH 4. The kinetics adsorption study followed the pseudo-first order. The isotherm adsorption study followed the Langmuir model. Based on the kinetics and isotherm study, the adsorption study of methylene blue and methyl red is chemical sorption.

**ARTICLE HISTORY**
Received: 14 Jul 2023
Revised: 29 Sep 2023
Accepted: 3 Oct 2023

**KEYWORDS**
Activated carbon
Silver composite
Spent coffee grounds
Methylene blue
Methyl red

## INTRODUCTION

Dye effluents from the textile, fabric, and paint industries are the primary causes of pollution in the aquatic environment. More than 10,000 textile dyes are produced in 70 million tons per year worldwide, and 5–10% of color effluents are over in waste disposal sites [1]. Dyes contaminated in the environment contain chemicals that have a toxic effect on microbes and animals, even harmful to humans, such as inhalation problems, carcinogens, and death if exposed continuously [2]. Methylene blue (MB) is a cationic dye ($C_{16}H_{18}N_3ClS$; 319.85 g/mol), and Methyl red (MR) is an anionic dye ($C_{15}H_{15}N_3O_2$; 269.30 g/mol) soluble in water, alcohol, and acetic acid. The dye removal process is often difficult due to its high solubility in water and non-biodegradable [3]. Moreover, molecules of dyes can prevent sunlight into the water body, thereby affecting the dissolved oxygen levels in the water and also increasing the chemical oxygen demand (COD) and biochemical oxygen demand (BOD) of the contaminated water body [4].

Several methods have been used to remove textile dyes from water, such as ion exchange resins, reverse osmosis, and nanofiltration. However, this method requires high operating costs, complex instruments, high energy consumption, and long processing times [5]. Comparatively, the adsorption technique is considered better in water treatment applications due to its simple design, convenience, and ease of operation. In addition, adsorption techniques can remove or minimize various types of pollutants, thus having a wider application in water pollution control [6]. Recently, adsorbent materials from composites and activated carbon with biomass waste precursors have been widely applied to dye effluents. These materials are environmentally friendly, easy to operate, and cost-effective. Metal composites have applications in materials science, catalysts, and environmental remediation. Green synthesis can synthesize metal composite, such as irradiation microwave. This method has advantages such as shorter reaction times, utilizing waste biomass constituents as reducing and stabilizing agents, good dispersion of nanoparticles, and high thermal stability [7]. Silver nanoparticles (AgNPs) have reacted with activated carbon to increase the functionality of materials. AgNPs are known to increase the surface of atoms [8].

Activated carbon is an adsorbent that is generally widely used for waste treatment and purification of pollutants in water. Activated carbon has advantages such as high surface area, micropores, high reactivity, high mechanical strength, and high adsorption capacity [6]. However, the industry currently prohibits the widespread use of commercial activated carbon due to the high cost and complex production process, where the raw materials used are derived from non-renewable materials such as coal, lignite, and petroleum coke [9]. Therefore, innovation is needed to produce metal composites and activated carbon based on biomass waste. A high percentage lignin content of 30% causes activated carbon to have a high carbon content and low ash [10]. Activated carbon can be activated physically and chemically using the pyrolysis method. This method used high temperature (400–550°C) under inert conditions, and there are two stages, such as carbonization and activation. The chemical that can be used as an active agent is phosphoric acid ($H_3PO_4$). It can increase the selectivity and adsorption capacity. The advantage of this method is that it can produce more results and better quality than other methods [11]. Various adsorbents with low production costs have been

*CORRESPONDING AUTHOR | Hafiizh Prasetia | ✉ hafiizh.prasetia@gmail.com

discovered but exhibit little adsorption potential for pollutant removal compared to commercial activated carbon. This is one of the main motivations for developing adsorbent materials that can efficiently remove and minimize pollutants.

Besides that, biomass waste is another cause of environmental pollution. Based on data from the United States Department of Agriculture (USDA), more than 150 million coffee of 60 kg of coffee bags were produced during the period 2012–2013, whereas 1 ton of coffee is known to produce more than 600 kg of waste by-products [12]. However, the by-products of the coffee production process have not been properly utilized. Spent coffee grounds contain chemical components such as water, protein, lipids, carbohydrates, ash content, amino acids, fatty acids, minerals, phenolic acids, and organic acids. Phenolic acids and organic acids are antioxidant compounds that contain lots of OH groups. In contrast, generally, phenolic and organic compounds contained in biomass waste can be used as bioreductor in the silver nanoparticle synthesis process [13].

MB and MR can be removed using a silver composite and activated carbon because these dyes contain a positive ion charge. Surface mass transfer and intraparticle diffusion occur between the composite material and the dye. Furthermore, activated carbon is a supporting medium for silver nitrate ($AgNO_3$) to increase the affinity for dye binding, making the process more stable. The advantages of these two materials (activated carbon from coffee grounds waste and $AgNO_3$) are that they can support each other and are suitable to effectively and efficiently remove MB and MR [14]. Silver composite and activated carbon from spent coffee grounds have a cross-linked mechanism between activated carbon and $AgNO_3$. Silver can diffuse into the pores of the activated carbon and change the interaction between MB and MR and the surface of activated carbon. The presence of activation with a chemical precursor also affects the selectivity of dye adsorption. Simultaneous activation and carbonization processes during the chemical activation at lower temperatures result in a better porous structure of activated carbon. Changes in material characteristics are one of the factors in increasing adsorbent performance. Research related to the use of spent coffee grounds as an adsorbent for methylene blue and methyl red adsorption has been done to increase the effectiveness and efficiency of dye adsorption in waters. However, the studies that have been carried out are necessary to consider in connection with preliminary tests to determine the maximum adsorption capacity of dyes and the renewability of biomass waste as a medium for the natural reduction process. Therefore, further research was carried out using spent coffee grounds through silver composites and activated carbon as adsorbents to overcome dye waste pollution.

## EXPERIMENTAL METHOD

### Materials and Instruments

Materials used in this study include Lampung Robusta Coffee, silver nitrate ($AgNO_3$) (Merck), methylene blue $C_{16}H_{18}N_3ClS$ (Merck), methyl red $C_{15}H_{15}N_3O_2$ (Merck), phosphoric acid ($H_3PO_4$) (Merck), and distilled water. Instruments used in this study include microwave irradiation digestion system MARS 6 for the synthesis of silver composite, test sieve shaker 100 mesh (± 75 µm) and 325 mesh (± 45 µm) for particle size reduction, Lindberg/Blue M 1200°C Split-Hinge Tube Furnaces for pyrolyze process of activated carbon, UV-Vis spectrophotometer thermo scientific GENESYS 10 for identification of absorbance spectra. Fourier-transform infrared spectroscopy (FTIR) Bruker-Tensor II ATR for analysis of functional groups in the chemical compound, and field emission scanning electron microscopy with energy dispersive X-ray spectroscopy (FESEM-EDX) Thermo Scientific Quattro S JIB-4610F for identification of morphology and element in the materials.

### Method and Procedure

The silver composite and activated carbon from spent coffee grounds were made based on the research of Omo-Okoro et al. [15] with slight modifications. Lampung Robusta Coffee of as much as 1 kg was extracted with 500 mL of hot distilled water for 24 hours. The extract of spent coffee ground as much as 500 g was dried at 115°C for 4 hours, then sifted using a test sieve shaker 325 mesh (± 45 µm). Furthermore, 10 mM $AgNO_3$ was added to 1 gram of spent coffee grounds in the 50 mL distilled water. In this step, the process of silver composite synthesis via extract spent coffee ground was carried out by microwave irradiation digestion system MARS 6 with a set of temperature 100°C, power 800 watts, and time 60 minutes. The silver composite-spent coffee ground (Ag-SCG) was dried at 110°C for 2 hours, then sifted using a test sieve shaker 325 mesh (± 45 µm).

The activated carbon from Ag-SCG (Ag-SCG/AC) was made by mixing 10 grams of Ag-SCG with 30 mL of 85% phosphoric acid solution (1:3). The mixture formed was stirred until homogeneous using a magnetic stirrer and left for 24 hours. The mixture sample was dried at 110°C for 2 hours. Furthermore, that sample was pyrolyzed in the tubular furnace under inert gas at 500°C for 1 hour. The activated carbon was washed with hot distilled water until the pH was neutral and dried at 110°C for 2 hours, then sifted with a 100 mesh (± 75 µm) shaker.

The adsorption of methylene blue (MB) and methylene red (MR) was carried out by batch method using a shaker incubator. The experiment was carried out with parameters of initial MR concentration of 25 mg/L, pH of 4 and 9, volume of 50 mL, adsorbent dose of 125 mg, contact time of 120 minutes, temperature of 36°C, and agitation speed of 120 rpm. The solution of MB and MR after the adsorption process was analyzed by UV-Vis spectrophotometer on the lambda maximum of 665 nm (MB) and 431 nm (MR). The initial MB and MR concentration (25 mg/L) and contact time (10, 20, 30, 60, 90, and 120 minutes) determined the kinetics and isotherm studies.

## RESULT AND DISCUSSION

The functional groups of spent coffee grounds (SCG), silver-spent coffee grounds composite (Ag-SCG), and activated carbon from silver-spent coffee grounds composite (Ag-SCG/AC) can be seen in Figure 1. There are seven functional groups in the SCG and Ag-SCG and six functional groups in the Ag-SCG/AC. The infrared (IR) spectra showed broad peaks between 3600–3200 $cm^{-1}$ indicating O–H vibration, two sharp peaks between 3000–2800 $cm^{-1}$ indicating C–H symmetric vibrations, C=O bond vibration appears on 1700–1600 $cm^{-1}$, C–O bond vibration appears on 1135–952 $cm^{-1}$ [16]. In addition, C=C bonds in aromatic rings appear between 1660–1560 $cm^{-1}$, C–C bonds in coffee grounds appear between 1586–1510 $cm^{-1}$ and C–H symmetric bonds occur between 750 ± 20 $cm^{-1}$ [17]. The IR spectra of Ag-SCG showed Ag–O bending at 570–550 $cm^{-1}$ [18]. The IR spectra of Ag-SCG/AC showed the interaction between Ag and O–P–O bending at 670–500 $cm^{-1}$ [19]. The IR spectra also showed several peak shifts and the intensity of band shape changes in the fingerprint zone at 1500–800 $cm^{-1}$. This confirmed that Ag-SCG and Ag-SCG/AC formed AgNPs and occurred reduction process of $Ag^{+}$ to $Ag^{0}$ due to the activity of phenolic compounds contained in SCG [20]. The phenolic compounds from natural resources have been used as green reagents to form and stabilize silver nanoparticles (AgNPs) due to the reducing ability of phenolic moieties and templating behavior [21]. Caffeic acid is a phenolic compound with excellent reduction ability due to its di-hydroxylic aromatic ring that contributes to the antioxidant activity of the molecule [22]. The antioxidant activity leads to the $Ag^{+}$ to $Ag^{0}$ reduction process [23].

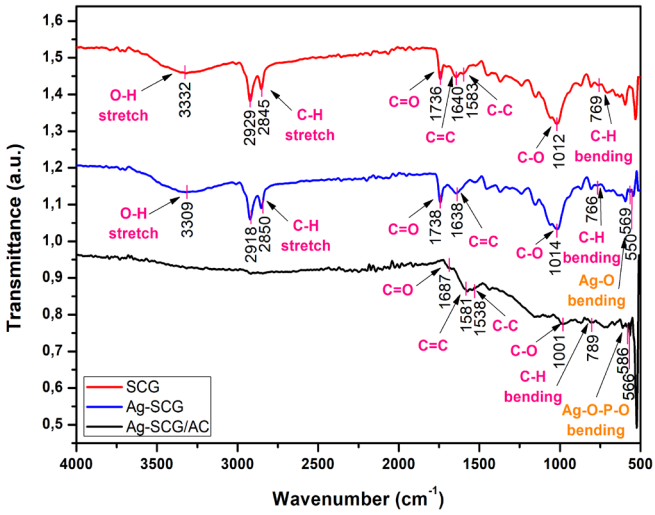


**Figure 1.** Fourier-transform infrared spectroscopy (FTIR) spectra of SCG and Ag-SCG/AC

The morphology and element content of Ag-SCG and Ag-SCG/AC can be seen in Figure 2 and Figure 3, respectively. The field emission scanning electron microscopy (FESEM) morphology of the two materials showed a porous and irregular polygonal shape. The results of the energy dispersive X-ray spectroscopy (EDX) spectrum showed elements of Ag-SCG and Ag-SCG/AC, such as C, O, Ag, and P. The At% of Ag from Ag-SCG is 2.2%, while Ag-SCG/AC is 0.6%. The At% of the Ag-SCG and Ag-SCG/AC materials have very different values, whereas the At% of Ag-SCG/AC has a lower value than Ag-SCG. This is due to the fast pyrolysis and chemical activation using phosphoric acid ($H_3PO_4$). Those processes facilitated cross-linking to form bonds such as polyphosphate esters, thus interacting with $Ag^{0}$ to form silver polyphosphate esters bonds [24]. Moreover, the At% of Ag has a smaller amount than the At% of C. This is due to the carbonization process increasing the At% amount of carbon and decreasing the At% amount of other substances due to heating at high temperatures [25].

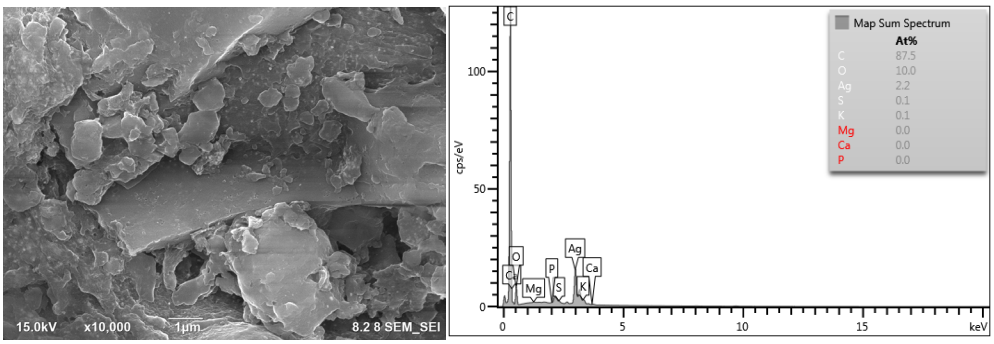


**Figure 2.** FESEM morphology and EDX spectrum of Ag-SCG

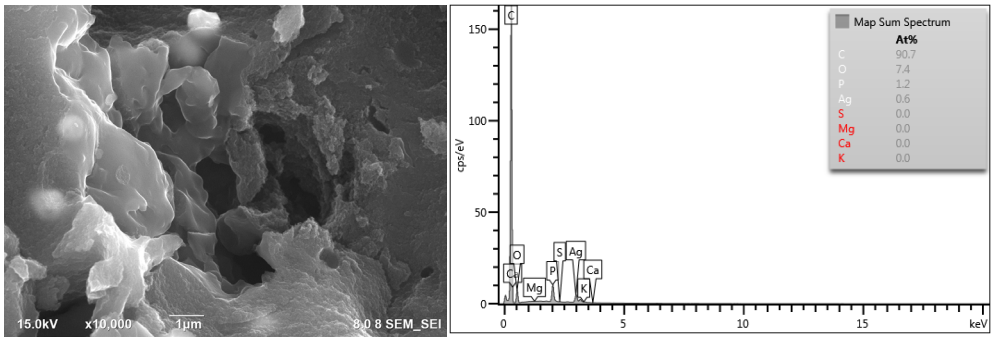


**Figure 3.** FESEM morphology and EDX spectrum of Ag-SCG/AC

The study of MB and MR adsorption on SCG, SCG/AC, Ag-SCG, and Ag-SCG/AC can be seen in Figure 4. The efficiency removal and adsorption capacity equations are respectively given as Equation (1) and (2):

$$\%\text{Removal} = \frac{C_i - C_e}{C_i} \times 100 \quad (1)$$

$$Q_e = (C_i - C_e) \times \frac{V}{M} \quad (2)$$

where $Q_e$ is the quantity of dye in the equilibrium (mg/g), $C_i$ and $C_e$ are, respectively, the initial concentration and equilibrium time of dye (mg/L), V is the volume of the solution, and M is the mass of the adsorbent.

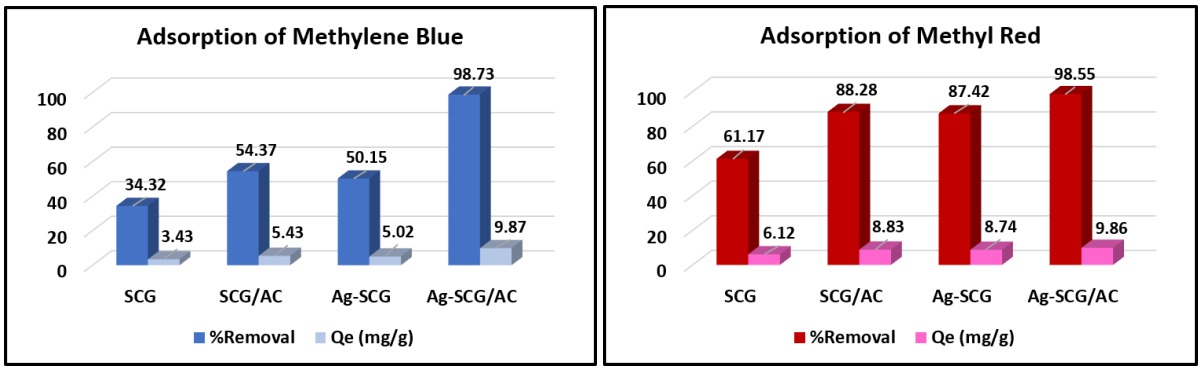


**Figure 4.** Removal efficiency and adsorption capacity of MB and MR on SCG, Ag-SCG, and Ag-SCG/AC

Based on the MB and MR adsorption results on SCG, SCG/AC, Ag-SCG, and Ag-SCG/AC materials, it was found that Ag-SCG/AC material has the highest efficiency removal and adsorption capacity of MB and MR, where 98.73% and 98.55%, respectively. MB adsorption has a significant effect after pyrolysis (50.15% to 98.73%), while MR adsorption does not have a significant effect after pyrolysis (87.42% to 98.55%). This is due to the influence of the pH used for MB and MR adsorption. MB can be significantly adsorbed using basic pH [26], while MR has two types of adsorption tendencies at both acidic and basic pH [27]. MR adsorption by Ag-SCG and Ag-SCG/AC materials are known to have insignificant increases in efficiency removal. This is possible in the 2-hour adsorption process where the pH changes from acidic to basic so that the structure of the methyl red molecule changes and becomes reactive towards the active site on the surface of the Ag-SCG and Ag-SCG/AC materials [27]. Furthermore, the materials after pyrolysis, such as SCG/AC and Ag-SCG/AC, have a high-efficiency removal due to the large surface area and abundance of large pores [28]. The Ag-SCG/AC material can remove MB and MR dyes effectively and efficiently. In this experiment, the efficiency removal and adsorption capacity of MR is slightly different than MB due to the difference of pH in the dye adsorption, the characteristics of the adsorbent, and the adsorption mechanism [29].

Ag-SCG/AC material is known to have high selectivity to remove MB and MR dyes in the aqueous medium. Adsorption occurs due to the electrostatic interaction between the $=N^+H$ group in the MB and MR dyes (positive dipole) with the O–P–O functional group of Ag-SCG/AC material (negative dipole) [30]. Besides that, in the Ag-SCG and Ag-SCG/AC materials, $Ag^0$ particles diffused into the pores of the material. Ag particles are known to improve the adsorption performance of dyes in the Ag-SCG and Ag-SCG/AC materials. The $Ag^0$ particles that interacted with SCG are known to increase the energy and surface area of the material [8]. Therefore, silver nitrate ($AgNO_3$) addition into Ag-SCG and Ag-SCG/AC materials can increase the removal efficiency and adsorption capacity of MB and MR dyes. Furthermore, Ag-SCG/AC material is used in the adsorption study due to the high-efficiency removal and high adsorption capacity for MB and MR dyes.

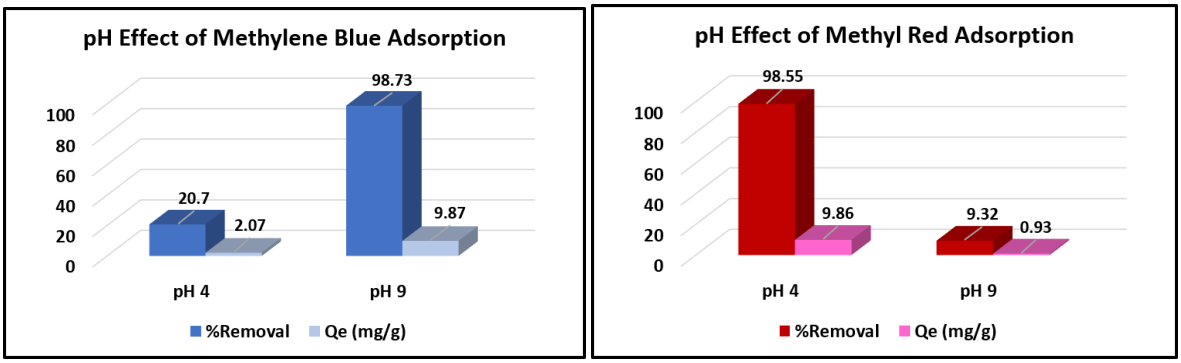


**Figure 5.** The pH effect of MB and MR adsorption on Ag-SCG/AC

In this preliminary study, pH 9 is used for the adsorption of methylene blue, and pH 4 is used for the adsorption of methyl red because it is the optimum pH based on the research results of Maia et al. and Khan et al. [3]. In methylene blue adsorption, pH below 4 has very small adsorption efficiency and adsorption capacity, while pH above 7 has large adsorption efficiency and adsorption capacity and is optimum at pH 9 [31]. Meanwhile, in methyl red adsorption, a pH below 4 has a large adsorption efficiency and adsorption capacity but reaches optimum at pH 4. Then, for a pH above 4, the adsorption efficiency and capacity are very small, not reaching 50% [3]. The pH effect of MB and MR adsorption can be seen in Figure 5. Based on those results, MB adsorption on Ag-SCG/AC occurred at pH 9, while MR adsorption was at pH 4. This is in accordance with research conducted by Maia et al. that MB can be adsorbed well at alkaline pH [31]. Meanwhile, MR can be adsorbed well at acidic pH based on Khan et al. research [3]. The performance of the activated carbon to remove MB is better than MR due to the molecular size of MB being higher than MR, thus having a lot of amine and carboxyl groups that interact with the active sites of the surface material. In addition, the adsorption of MB and MR occurred by the interaction between the material that has a negative charge and the dye molecules that have a positive charge. Therefore, the characteristics of the adsorbent and the pH of dyes are the important variables that can affect the adsorption process. The MB and MR adsorption mechanism can be studied further in kinetics and isotherm adsorption.

The kinetics study of MB and MR on Ag-SCG/AC material can be seen in Figure 6. In this experiment, we used two types of kinetics models: pseudo-first order and pseudo-second order. The linear kinetics of pseudo-first order and pseudo-second order equations are respectively given as Equation (3) and Equation (4):

$$\ln\left(\frac{C_0}{C_t}\right) = k_1 \times t \tag{3}$$

$$\frac{t}{Q_t} = \frac{1}{k_2 Q_e^2} + \frac{t}{Q_e} \tag{4}$$

where $Q_e$ is the quantity of dye in the equilibrium (mg/g), $C_0$ and $C_e$ are, respectively, the initial concentration and equilibrium time of dye (mg/L), $Q_t$ is the quantity of dye at the time of t (mg/g), t is time (min), $k_1$ is pseudo-first order equilibrium rate constant (1/min), and $k_2$ is pseudo-second order equilibrium rate constant (1/min).

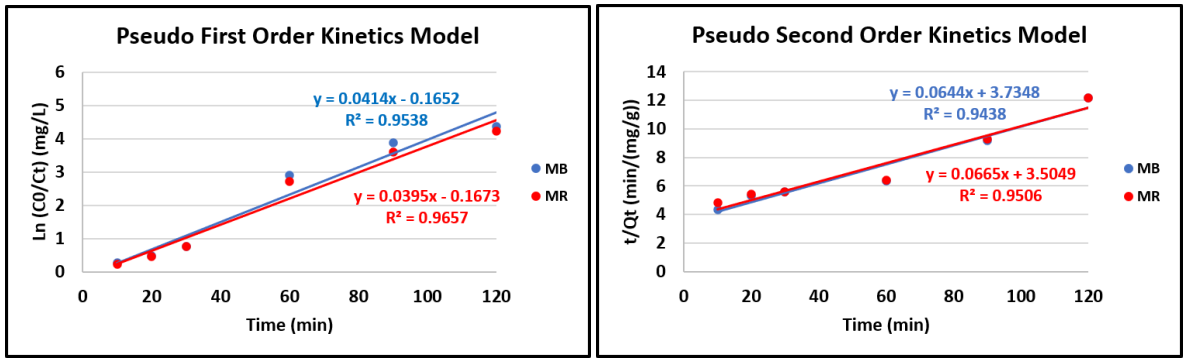


**Figure 6.** Kinetics of pseudo-first order and pseudo-second order for MB and MR adsorption on Ag-SCG/AC

Based on the kinetics study of MB and MR results on the Ag-SCG/AC material, it is known that MB and MR adsorption follow the pseudo-first-order. It assumed that one dye molecule is adsorbed onto one active site on the surface adsorbent material [3]. The value of the $R^2$, equilibrium rate constant ($k_1$ and $k_2$), and quantity of dyes that adsorbed at equilibrium ($Q_e$) can be seen in Table 1. The plot between t/Qt versus t at pseudo-second order kinetics in the MB and MR adsorption gives a line with poor linear regression coefficient ($R^2$), where 0.9438 and 0.9506, respectively. Meanwhile, the plot between $\ln(C_0/C_t)$ versus t at pseudo-first order kinetics gives the best $R^2$ coefficient, where 0.9538 and 0.9657, respectively.

**Table 1.** Kinetics of pseudo-first order and pseudo-second order for MB and MR adsorption

| Dyes | Pseudo First Order | | | Pseudo Second Order | | |
|---|---|---|---|---|---|---|
| | $R^2$ | $k_1$ (1/min) | $Q_e$ (mg/g) | $R^2$ | $k_2$ (1/min) | $Q_e$ (mg/g) |
| **MB** | 0.9538 | 0.0953 | 0.7820 | 0.9438 | 1.1132 | 0.2678 |
| **MR** | 0.9657 | 0.0910 | 0.7765 | 0.9506 | 1.2241 | 0.2853 |

The isotherm study of MB and MR on Ag-SCG/AC material can be seen in Figure 7. In this experiment, we used two types of isotherm models, such as the Langmuir and Freundlich models. The linear isotherm of Langmuir and Freundlich equations are respectively given as Equation (5) and Equation (6):

$$\frac{C_e}{Q_e} = \frac{1}{Q_m K_L} + \frac{C_e}{Q_m} \quad (5)$$

$$\ln Q_e = \ln K_F + \frac{1}{n_f} \ln C_e \quad (6)$$

where $Q_e$ is the quantity of dye in the equilibrium (mg/g), $C_e$ is the concentration of dye at equilibrium time (mg/L), $Q_m$ is the maximum adsorption capacity (mg/g), $n_f$ is the adsorption intensity, $K_L$ is the Langmuir equilibrium rate constant (L/mg), and $K_F$ is the Freundlich equilibrium rate constant (L/mg).

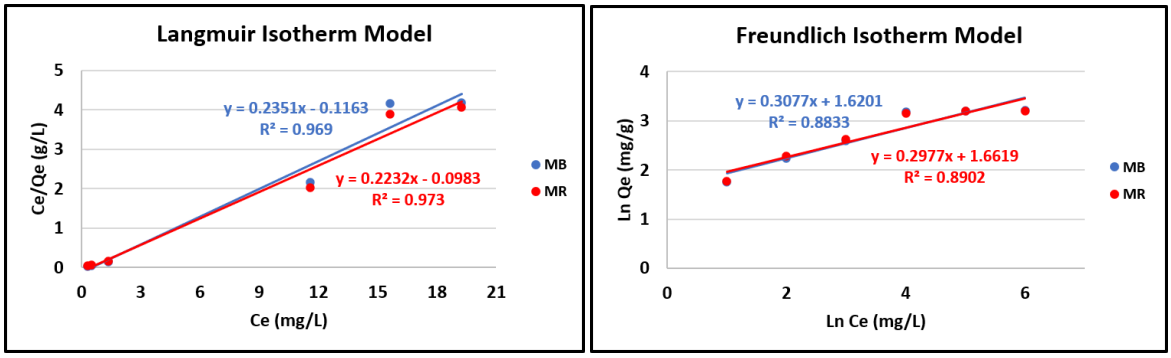


**Figure 7.** Isotherm model of Langmuir and Freundlich for MB and MR adsorption on Ag-SCG/AC

Based on the isotherm study of MB and MR results on the Ag-SCG/AC material, it is known that MB and MR adsorption follows the Langmuir model. This isotherm model explains monolayer homogeneous adsorption [32]. The value of the $R^2$, equilibrium rate constant ($K_L$ and $K_F$), $Q_m$, and $n_f$ can be seen in Table 2. The plot between ln $Q_e$ versus ln $C_e$ at Freundlich model in the MB and MR adsorption gives a line with poor linear regression coefficient ($R^2$), where 0.8833 and 0.8902, respectively. Meanwhile, the plot between $C_e/Q_e$ versus $C_e$ at the Langmuir model gives the best $R^2$ coefficient, where 0.9690 and 0.9730, respectively. The Langmuir isotherm included a chemical adsorption process identical to the strong interaction between the adsorbate and the adsorbent [33].

**Table 2.** Isotherm model of Langmuir and Freundlich for MB and MR adsorption

| Dyes | Langmuir Model | | | Freundlich Model | | |
|---|---|---|---|---|---|---|
| | $R^2$ | $K_L$ (L/mg) | $Q_m$ (mg/g) | $R^2$ | $K_F$ (L/mg) | $n_f$ |
| **MB** | 0.9690 | 0.4947 | 4.2535 | 0.8833 | 0.4825 | 0.3077 |
| **MR** | 0.9730 | 0.4404 | 4.4803 | 0.8902 | 0.5080 | 0.2977 |

## CONCLUSION

The activated carbon from silver-spent coffee grounds composite (Ag-SCG/AC) material has a porous and irregular polygonal shape. The infrared (IR) spectra of Ag-SCG/AC contained two peaks between 670–500 $cm^{-1}$ that indicated O–P–O groups (negative charge), which can interact with dye molecules (positive charge). The pH of dyes and characteristics of adsorbent affect the efficiency removal and adsorption capacity. The best efficiency removal in this study was achieved at pH 9 and 4 with 98.73% and 98.55% adsorption for methylene blue (MB) and methylene red (MR), respectively. The kinetics study followed pseudo-first order, and the isotherm study followed the Langmuir model that indicated chemical sorption.

## ACKNOWLEDGEMENT

The authors would like to thank analytical groups in the Research Center for Chemistry, BRIN, for the cooperation in using its Laboratory and equipment for analysis.

## REFERENCES

[1] M. Rafatullah, O. Sulaiman, R. Hashim, and A. Ahmad. "Adsorption of methylene blue on low-cost adsorbents: A review." *J. Hazard. Mater.*, vol. 177, no. 1–3, pp. 70–80, 2010.

[2] B. H. Hameed and F. B. M. Daud. "Adsorption studies of basic dye on activated carbon derived from agricultural waste: *Hevea brasiliensis* seed coat." *Chem. Eng. J.*, vol. 139, no. 1, pp. 48–55, 2008.

[3] E. A. Khan, Shahjahan, and T. A. Khan. "Adsorption of methyl red on activated carbon derived from custard apple (*Annona squamosa*) fruit shell: Equilibrium isotherm and kinetic studies." *J. Mol. Liq.*, vol. 249, pp. 1195–1211, 2018.

[4] R. Al-Tohamy, S. S. Ali, F. Li, K. M. Okasha, Y. A.-G. Mahmoud, T. Elsamahy, H. Jiao, Y. Fu, and J. Sun. "A critical review on the treatment of dye-containing wastewater: Ecotoxicological and health concerns of textile dyes and possible remediation approaches for environmental safety." *Ecotoxicol. Environ. Saf.*, vol. 231, p. 113160, 2022.

[5] C. Flores, F. Ventura, J. Martin-Alonso, and J. Caixach. "Occurrence of perfluorooctane sulfonate (PFOS) and perfluorooctanoate (PFOA) in N.E. Spanish surface waters and their removal in a drinking water treatment plant that combines conventional and advanced treatments in parallel lines." *Sci. Total Environ.*, vol. 461–462, pp. 618–626, 2013.

[6] M. Sulyman, J. Namiesnik, and A. Gierak. "Low-cost adsorbents derived from agricultural by-products/wastes for enhancing contaminant uptakes from wastewater: A review." *Polish J. Environ. Stud.*, vol. 26, no. 2, pp. 479–510, 2017.

[7] P. Xu, X. Han, B. Zhang, Y. Du, and H. L. Wang. "Multifunctional polymer-metal nanocomposites via direct chemical reduction by conjugated polymers." *Chem. Soc. Rev.*, vol. 43, no. 5, pp. 1349–1360, 2014.

[8] S.-M. Li, N. Jia, M.-G. Ma, Z. Zhang, Q.-H. Liu, and R.-C. Sun. "Cellulose–silver nanocomposites: Microwave-assisted synthesis, characterization, their thermal stability, and antimicrobial property." *Carbohydr. Polym.*, vol. 86, no. 2, pp. 441–447, 2011.

[9] J. Nyirenda, G. Kalaba, and O. Munyati. "Synthesis and characterization of an activated carbon-supported silver-silica nanocomposite for adsorption of heavy metal ions from water." *Results Eng.*, vol. 15, no. August, p. 100553, 2022.

[10] M. Lewoyehu. "Comprehensive review on synthesis and application of activated carbon from agricultural residues for the remediation of venomous pollutants in wastewater." *J. Anal. Appl. Pyrolysis*, vol. 159, p. 105279, 2021.

[11] D. Gogoi, M. Kumar, and Y. G. Lakshmi. "A comprehensive review on 'Pyrolysis' for energy recovery." *Bioenergy Res.*, no. January, 2023.

[12] F. Codignole Luz, M. Volpe, L. Fiori, A. Manni, S. Cordiner, V. Mulone, and V. Rocco. "Spent coffee enhanced biomethane potential via an integrated hydrothermal carbonization-anaerobic digestion process." *Bioresour. Technol.*, vol. 256, pp. 102–109, 2018.

[13] S. S. Arya, R. Venkatram, P. R. More, and P. Vijayan. "The wastes of coffee bean processing for utilization in food: A review." *J. Food Sci. Technol.*, vol. 59, no. 2, pp. 429–444, 2022.

[14] N. Dwivedi and S. Dwivedi. "Chapter 22 - Sustainable biological approach for removal of cyanide from wastewater of a metal-finishing industry," in *Membrane-Based Hybrid Processes for Wastewater Treatment*, M. P. Shah and S. B. T.-M.-B. H. P. for W. T. Rodriguez-Couto, Eds. Elsevier, 2021, pp. 463–479.

[15] P. N. Omo-Okoro, C. E. Maepa, A. P. Daso, and J. O. Okonkwo. "Microwave-assisted synthesis and characterization of an agriculturally derived silver nanocomposite and its derivatives." *Waste and Biomass Valorization*, vol. 11, no. 5, pp. 2247–2259, 2020.

[16] L. F. Ballesteros, J. A. Teixeira, and S. I. Mussatto. "Chemical, functional, and structural properties of spent coffee grounds and coffee silverskin." *Food Bioprocess Technol.*, vol. 7, no. 12, pp. 3493–3503, 2014.

[17] J. J. Gao, Y. B. Qin, T. Zhou, D. D. Cao, P. Xu, D. Hochstetter, and Y. F. Wang. "Adsorption of methylene blue onto activated carbon produced from tea (*Camellia sinensis* L.) seed shells: Kinetics, equilibrium, and thermodynamics studies." *J. Zhejiang Univ. Sci. B*, vol. 14, no. 7, pp. 650–658, 2013.

[18] M. R. H. Siddiqui, S. F. Adil, M. E. Assal, R. Ali, and A. Al-Warthan. "Synthesis and characterization of silver oxide and silver chloride nanoparticles with high thermal stability." *Asian J. Chem.*, vol. 25, no. 6, pp. 3405–3409, 2013.

[19] W. Jastrzębski, M. Sitarz, M. Rokita, and K. Bułat. "Infrared spectroscopy of different phosphates structures." *Spectrochim. Acta Part A Mol. Biomol. Spectrosc.*, vol. 79, no. 4, pp. 722–727, 2011.

[20] N. El-Desouky, K. Shoueir, I. El-Mehasseb, and M. El-Kemary. "Synthesis of silver nanoparticles using bio valorization coffee waste extract: Photocatalytic flow-rate performance, antibacterial activity, and electrochemical investigation." *Biomass Convers. Biorefinery*, no. 0123456789, 2022.

[21] A. A. Bhutto, Ş. Kalay, S. T. H. Sherazi, and M. Culha. "Quantitative structure–activity relationship between antioxidant capacity of phenolic compounds and the plasmonic properties of silver nanoparticles." *Talanta*, vol.

189, no. March, pp. 174–181, 2018.
[22] A. Scroccarello, B. M.-H. Junior, F. D. Pelle, J. Ciancetta, G. Ferraro, E. Fratini, L. Valbonetti, C. C. Copez, D. Compagnone. "Effect of phenolic compounds-capped AgNPs on growth inhibition of *Aspergillus niger*." *Colloids Surfaces B Biointerfaces*, vol. 199, no. September 2020, 2021.
[23] N. U. H. Altaf, M. Y. Naz, S. Shukrullah, M. Ghamkar, M. Irfan, S. Rahman, T. Jakubowski, E. A. Alqurashi, A. Glowacz, and M. H. Mahnashi. "Non-thermal plasma reduction of Ag+ ions into silver nanoparticles in open atmosphere under statistically optimized conditions for biological and photocatalytic applications." *Materials (Basel).*, vol. 15, no. 11, pp. 1–24, 2022.
[24] O. Oginni, K. Singh, G. Oporto, B. Dawson-Andoh, L. McDonald, and E. Sabolsky. "Effect of one-step and two-step H3PO4 activation on activated carbon characteristics." *Bioresour. Technol. Reports*, vol. 8, p. 100307, 2019.
[25] F. Ortega, L. Giannuzzi, V. B. Arce, and M. A. García. "Active composite starch films containing green synthetized silver nanoparticles." *Food Hydrocoll.*, vol. 70, pp. 152–162, 2017.
[26] I. Khan, K. Saeed, I. Zekker, B. Zhang, A. H. Hendi, A. Ahmad, S. Ahmad, N. Zada, H. Ahmad, L. A. Shah, T. Shah, and I. Khan. "Review on methylene blue: Its properties, uses, toxicity and photodegradation." *Water (Switzerland)*, vol. 14, no. 2, 2022.
[27] L. I. U. Qiong, C. Yu-miao, and L. I. U. Zhao-qing. "Determination of acid dissociation constant of methyl red by multi-peaks gaussian fitting method based on UV-Visible absorption spectrum," vol. 28, no. 5, pp. 1030–1036, 2012.
[28] T. Q. Tuan, N. V. Son, H. T. K. Dung, N. H. Luong, B. T. Thuy, N. T. V. Anh, N. D. Hoa, and N. H. Hai. "Preparation and properties of silver nanoparticles loaded in activated carbon for biological and environmental applications." *J. Hazard. Mater.*, vol. 192, no. 3, pp. 1321–1329, 2011.
[29] J. M. Gómez, J. Galán, A. Rodríguez, and G. M. Walker. "Dye adsorption onto mesoporous materials: pH influence, kinetics and equilibrium in buffered and saline media." *J. Environ. Manage.*, vol. 146, pp. 355–361, 2014.
[30] A. Molla, Y. Li, B. Mandal, S. G. Kang, S. H. Hur, and J. S. Chung. "Selective adsorption of organic dyes on graphene oxide: Theoretical and experimental analysis." *Appl. Surf. Sci.*, vol. 464, pp. 170–177, 2019.
[31] L. S. Maia, A. I. C. da Silva, E. S. Carneiro, F. M. Monticelli, F. R. Pinhati, and D. R. Mulinari. "Activated carbon from palm fibres used as an adsorbent for methylene blue removal." *J. Polym. Environ.*, no. 0123456789, 2020.
[32] E. G. Lemraski and Z. Palizban. "Comparison of 2-amino benzyl alcohol adsorption onto activated carbon, silicon carbide nanoparticle and silicon carbide nanoparticle loaded on activated carbon." *J. Mol. Liq.*, vol. 212, pp. 245–258, 2015.
[33] P. Pourhakkak, A. Taghizadeh, M. Taghizadeh, M. Ghaedi, and S. Haghdoust. "Chapter 1 - Fundamentals of adsorption technology," in *Adsorption: Fundamental Processes and Applications*, M. Ghaedi, Ed., in Interface Science and Technology, vol. 33. Elsevier, 2021, pp. 1–70.